

Excitation wavelength dependence of energy transfer in dye mixture doped polymer optical fibre preforms

M. Kailasnath^{a,*}, Nishant Kumar^b, V.P.N. Nampoora^a, C.P.G. Vallabhan^b, P. Radhakrishnan^a

^a International School of Photonics, Cochin University of Science and Technology, Kochi 682022, India

^b Centre of Excellence in Lasers and Optoelectronic Sciences, Cochin University of Science and Technology, Kochi 682022, India

ARTICLE INFO

Article history:

Received 27 February 2008

Received in revised form 21 May 2008

Accepted 30 May 2008

Available online 22 June 2008

Keywords:

Optical fibre preform

Energy transfer

Methyl methacrylate

Fluorescence

ABSTRACT

Dependence of energy transfer parameters on excitation wavelength has been investigated in poly (methyl methacrylate) (PMMA) optical fibre preforms doped with C 540:Rh B dye mixture by studying the fluorescence intensity and the lifetime variations. A fluorescence spectrophotometer was used to record the excitation spectra of the samples for the emission wavelengths 495 and 580 nm. The fluorescence emission from the polymer rods was studied at four specific excitation wavelengths viz; 445, 465, 488 and 532 nm. The fluorescence lifetime of the donor molecule was experimentally measured in polymer matrix by time correlated single photon counting technique. The energy transfer rate constants and transfer efficiencies were calculated and their dependence on the acceptor concentration was analysed for three excitation wavelengths. It was found that any change in the excitation wavelength leads to significant variations in the quenching characteristics, which in turn affect the calculated energy transfer parameters.

© 2008 Elsevier B.V. All rights reserved.

1. Introduction

Intermolecular energy transfer between two distinct molecular species in the condensed phase has been observed in numerous molecular systems [1]. Following the introduction of dye lasers, energy transfer between dye molecules has been used to exploit the absorption properties of a lasing dye mixture for matching with the emission spectrum of the optical pump source. The primary motivation for the use of mixture of dyes as lasing medium was either an improvement in the laser performance or the possibility of multi-frequency operation [2]. Even though a number of techniques exist for obtaining two or more wavelengths simultaneously from a single dye laser, they use several wavelength selective elements in the dye laser cavity [3–5]. The use of dye mixture doped transparent polymers in solid-state dye lasers and polymer optical fibre amplifiers can be a very good method to extend these conventional approaches.

One of the important advantages of transparent polymers compared to the traditional optical materials is that it is possible to introduce organic dyes or other compounds that can play the role of active components into the polymers, which appreciably changes the characteristics of the polymer matrix [6,7]. Optical amplifiers and lasers made of dye-doped fiber require much less pump power

compared with bulk material because of the effective confinement and long interaction length available in the fiber. Since photobleaching increases with the increase of the exposure intensity, low pump intensity would increase the lifespan of the gain medium. Also, the thin and long geometry of the fiber is ideal for good thermal relaxation so as to minimize the thermally induced photobleaching [8]. Recently, we have observed an enhancement in the radiative energy transfer efficiency in the polymer phase of C 540:Rh B dye mixture compared to monomer when excited with a 445 nm laser beam [9]. However, the emission wavelengths and relative intensities can vary with excitation wavelength in such cases. In the present study, we discuss the excitation wavelength dependence of the fluorescence emission and energy transfer mechanism using coumarin 540 dye as donor in C 540:Rh B dye mixture doped PMMA rods.

2. Theory

Detailed theory of energy transfer dye laser is discussed elsewhere [10]. The rate constants for the radiative and nonradiative energy transfer mechanisms are given by Stern-Volmer plots given by the equations

$$\frac{I_{0d}}{I_d} = 1 + K\tau_{0d}[A] \quad (1)$$

$$\frac{\varphi_{0d}}{\varphi_d} = 1 + K_{nr}\tau_{0d}[A] \quad (2)$$

* Corresponding author. Tel.: +91 4842575848; fax: +91 4842576714.
E-mail address: kailas@cusat.ac.in (M. Kailasnath).

where I_{0d} and I_d are the fluorescence intensities of the donor in the absence and presence of acceptor respectively while, ϕ_{0d} and ϕ_d are corresponding quantum yields. τ_{0d} is the fluorescence lifetime of the donor without acceptor and $[A]$ is the acceptor concentration. K and K_{nr} are total and non-radiative transfer rate constants respectively. According to the Forster Dexter theory, the critical radius for resonant energy transfer between the donor and acceptor molecules are given by the expression [11]:

$$R_0 = [8.8 \times 10^{23} \kappa^2 n^{-4} \phi_{0d} J(\lambda)]^{1/6} (\text{\AA}) \quad (3)$$

where κ^2 is the dipole orientation factor, n is the refractive index of the medium, ϕ_{0d} is the fluorescence quantum yield of the donor in the absence of acceptor and $J(\lambda)$ is the spectral overlap integral given by

$$J(\lambda) = \int \varepsilon_A(\lambda) F_D(\lambda) \lambda^4 d\lambda (\text{cm}^3 \text{M}^{-1}) \quad (4)$$

where $\varepsilon_A(\lambda)$ is the extinction coefficient of acceptor and $F_D(\lambda)$ is the fluorescence emission intensity of the donor as a function of the total integrated intensity. Evidently, any variation in the values of $\varepsilon_A(\lambda)$ and $F_D(\lambda)$ will result in a corresponding change in the energy transfer parameters. However, the fluorescence emission spectrum is independent of excitation wavelength as long as the excitation wavelength is well within the absorption spectrum of the molecule. Hence $J(\lambda)$ will not have significant dependence on the donor excitation wavelength.

Experimentally, the critical transfer radius (R_0), for which energy transfer from the excited donor (D^*) to the acceptor $[A]$ and emission from D^* are equally probable, is given by [12]

$$R_0 = \frac{7.35}{([A]_{1/2})^{1/3}} \quad (5)$$

where $[A]_{1/2}$ is the half quenching concentration which can be obtained under the condition:

$$\frac{I_{0d}}{I_d} = 2$$

Total transfer efficiency η is written as the sum of two parts:

$$\eta = \eta_r + \eta_{nr} \quad (6)$$

As is well known, in the presence of acceptor, the fluorescence intensity of the donor is reduced from I_{0d} to I_d by energy transfer to acceptor. A more practical expression for η of an energy transfer dye laser (ETDL) system can be given by [13,14]:

$$\eta = 1 - \frac{I_d}{I_{0d}} \quad (7)$$

The nonradiative transfer efficiency η_{nr} is defined as [15]:

$$\eta_{nr} = \pi^{1/2} X \exp(X^2)(1 - \text{erf}X) \quad (8)$$

where X is the molar concentration expressed relative to the critical molar concentration of the acceptor.

3. Experimental

A series of dye mixture doped polymer rods were fabricated by the standard procedure for making the polymer optical fiber preforms without cladding [16]. The donor concentration was kept constant at 10^{-5} m/l whereas the acceptor concentration was varied from 4×10^{-5} to 7×10^{-4} m/l. The fluorescence emission from the rods was measured using a Varian Cary-Eclipse fluorescence spectrophotometer with excitation wavelengths 445, 465, 488 and 532 nm. Here, 445 nm is the longest excitation wavelength, which was found to be suitable for avoiding any direct excitation of



Fig. 1. A photograph of the fabricated preforms.

the acceptor molecules. The wavelength 488 nm coincides with the prominent argon ion laser emission but not well within the absorption spectrum of the donor while 532 nm matches with the frequency doubled Nd:YAG laser wavelength, which is at the absorption maximum of the acceptor molecule. Finally, 465 nm is an intermediate wavelength, which ensures a multiwavelength emission from the fabricated rods. The excitation spectra of the samples were also recorded in the fluorescence spectrophotometer for the peak emission wavelengths of 495 and 580 nm of the donor and acceptor, respectively. Optical absorption spectra of the samples were recorded on a Jasco V-570 spectrophotometer. The fluorescence lifetimes of the donor in pure form and in the presence of acceptor in PMMA matrix were measured using time-correlated single photon counting technique employing a micro channel plate photomultiplier tube (Hamamatsu R 3809 U-50) and a multichannel analyser. The measurement is made using an IBH-5000 Single Photon Counting Spectrometer. A nano-LED (Spectra Physics) emitting at 455 nm with a resolution of 200 ps was used as the excitation source. The fluorescence decay curves were analysed using an iterative fitting program provided by IBH and no further deconvolution was made.

4. Results and discussion

Fig. 1 shows the photograph of the fabricated polymer optical fiber preforms doped with dye mixture with varying acceptor concentrations. Individual absorption spectra of Rh B (10^{-4} mol/l) and C 540 (10^{-5} mol/l) in PMMA are presented in Fig. 2 along with the emission spectrum of C 540 with a 445 nm excitation. Since a considerable area under the emission line shapes of C 540 at 445 nm excitation overlaps with the absorption line shapes of Rh B, energy transfer from C 540 to Rh B is clearly possible, the extent of this being depended on the overlapping area. Fig. 3 depicts the net absorption spectra of the samples, which clearly shows that there are significant modifications in the absorption pattern with acceptor concentration. We attribute these changes in the absorption spectra as due to the process of energy transfer as well as due to the presence of aggregations like dimers and trimers in the samples.

The excitation spectrum of the rods at 495 nm, is depicted in Fig. 4. It is clear that there is a significant shift in the peak wavelength of excitation for emission at this wavelength with acceptor concentration. From the pure donor, efficient fluorescence can be expected at an excitation wavelength of about 475 nm. This value continuously reduces to 453 nm with an acceptor concentration of 6×10^{-4} m/l. With increasing acceptor concentration the long wavelength tail of the donor emission increasingly gets absorbed by the acceptor.

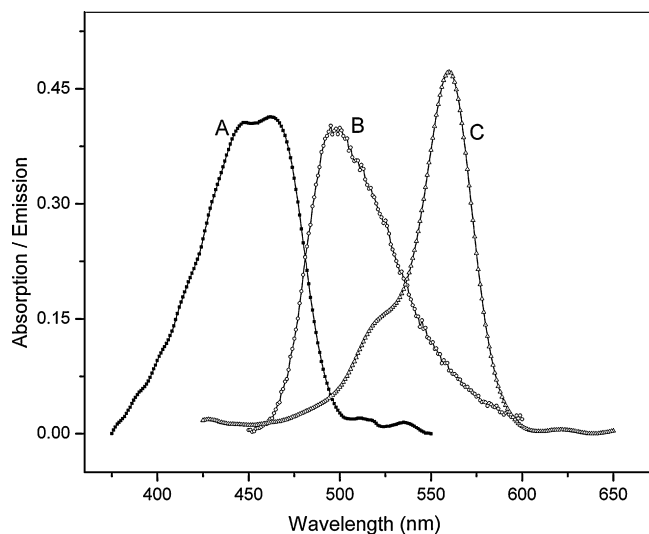


Fig. 2. Overlapping of absorption and emission spectra in PMMA matrix. (A) absorption spectrum of C 540, (B) emission spectrum of C 540 for 445 nm excitation and (C) absorption spectrum of Rh B.

Also there is no efficient wavelength of excitation for emission at 490 nm from the pure acceptor. Fig. 5a and b shows the excitation spectra of the samples at the emission maximum of the acceptor, i.e. 580 nm. A new peak appears in the excitation spectra in the 570–580 nm region. As shown in Figs. 6–8, the fluorescence spectrum of dye mixture exhibit double peak in the intermediate acceptor concentrations corresponding to characteristic donor and acceptor emission. The peak emission from the acceptor shift to higher wavelengths with increasing acceptor concentration [A] and it appears around 605 nm at highest [A]. In the excitation spectrum, at highest acceptor concentration as well as with pure donor, the sharp peak at 580 nm results from the scattering of the excitation radiation. At intermediate concentrations, there is fluorescence emission around 570–580 nm and the given peak is due to the resonant fluorescence under 580 nm excitation. At highest acceptor concentration, the peak is shifted to higher wavelength and the

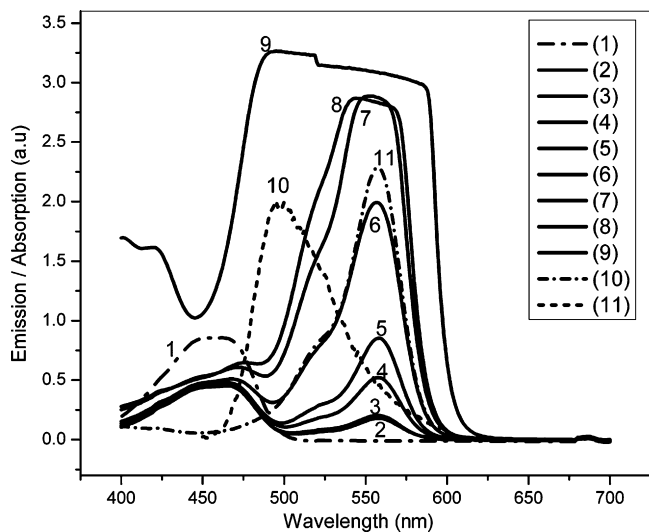


Fig. 3. Net absorption spectra of dye mixture doped PMMA rods along with pure donor emission. (1) Donor only (5×10^{-5} m/l), (2) $[A] = 4 \times 10^{-5}$, (3) $[A] = 7 \times 10^{-5}$, (4) $[A] = 10^{-4}$, (5) $[A] = 2 \times 10^{-4}$, (6) $[A] = 4 \times 10^{-4}$, (7) $[A] = 5 \times 10^{-4}$, (8) $[A] = 6 \times 10^{-4}$, (9) $[A] = 7 \times 10^{-4}$, (10) acceptor only (10^{-4} m/l), (11) donor emission.

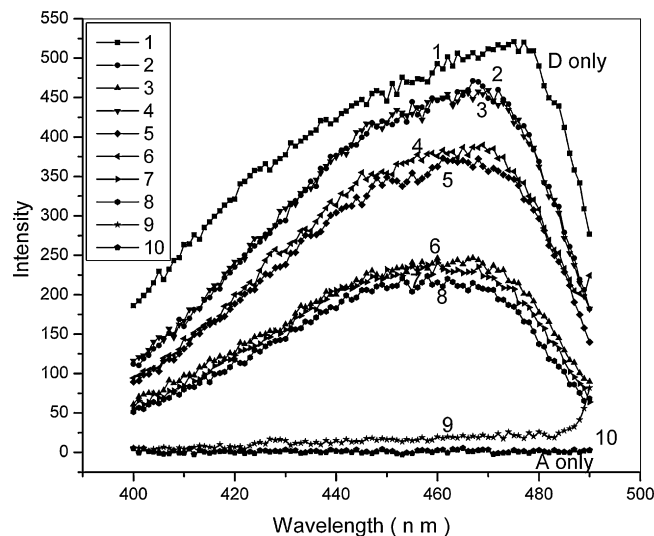


Fig. 4. Excitation spectra of dye mixture doped PMMA for 495 nm emission. (1) Donor only (5×10^{-5} m/l), (2) $[A] = 4 \times 10^{-5}$ m/l, (3) $[A] = 7 \times 10^{-5}$ m/l, (4) $[A] = 10^{-4}$ m/l, (5) $[A] = 2 \times 10^{-4}$ m/l, (6) $[A] = 4 \times 10^{-4}$ m/l, (7) $[A] = 5 \times 10^{-4}$ m/l, (8) $[A] = 6 \times 10^{-4}$ m/l, (9) $[A] = 7 \times 10^{-4}$ m/l and (10) acceptor only (10^{-4} m/l).

emission from this sample is no more around 580 nm. Evidently, the emission wavelength from this sample is beyond 600 nm as seen in the fluorescence spectra.

Fig. 6 indicates the available wavelengths that can be produced from the fabricated polymer rods with varying relative intensities for an excitation wavelength of 445 nm. In the present study we have noticed that both relative intensities and peak emission wavelengths are different at various excitation wavelengths. Figs. 7–9 represent the emission spectra for 465, 488 and 532 nm excitations respectively.

For the excitations at 445 and 465 nm, donor fluorescence shows a continuous blue shift of about 20 nm in the range of acceptor concentrations used in the present study. Meanwhile, the acceptor shows a continuous red shift of about 15 nm up to $[A] = 5 \times 10^{-4}$ m/l which is then blue shifted by about 5 nm. Beyond this [A] value, the acceptor emission was red shifted.

In the absence of donor, the acceptor showed a continuous red shift of about 13 nm. It may be pointed out that the pure acceptor has no emission with 445 and 465 nm excitations even though there is a little emission for 488 nm excitation. For 488 nm excitation, we could not notice much blue shift for the donor but the acceptor emission was again red shifted by about 15 nm.

These results for the 445 and 465 nm excitations are in good agreement with our earlier investigation on the wavelength shifts with a 445 nm laser excitation [9].

At an optimum concentration of the acceptor for the energy transfer, the acceptor emission shows a blue shift. The donor-sensitized system was observed to have a higher gain compared to an unsensitized system due to an increase in the effective lifetime. As a result of this, the gain maximum is shifted to the blue region [17,18]. At higher acceptor concentrations, this effect was absent because of the dominance of collisional de-excitation. At 488 nm, there were no significant blue shifts from both donor and acceptor. At this wavelength donor excitation is not much efficient and there is a possibility for the direct excitation of the acceptor as well. The 532 nm excitation was found to be absorbed by acceptor alone and the corresponding emission showed a continuous red shift of about 15 nm. Fig. 10 shows the variations of the simultaneous emission wavelengths exhibited by the rods.

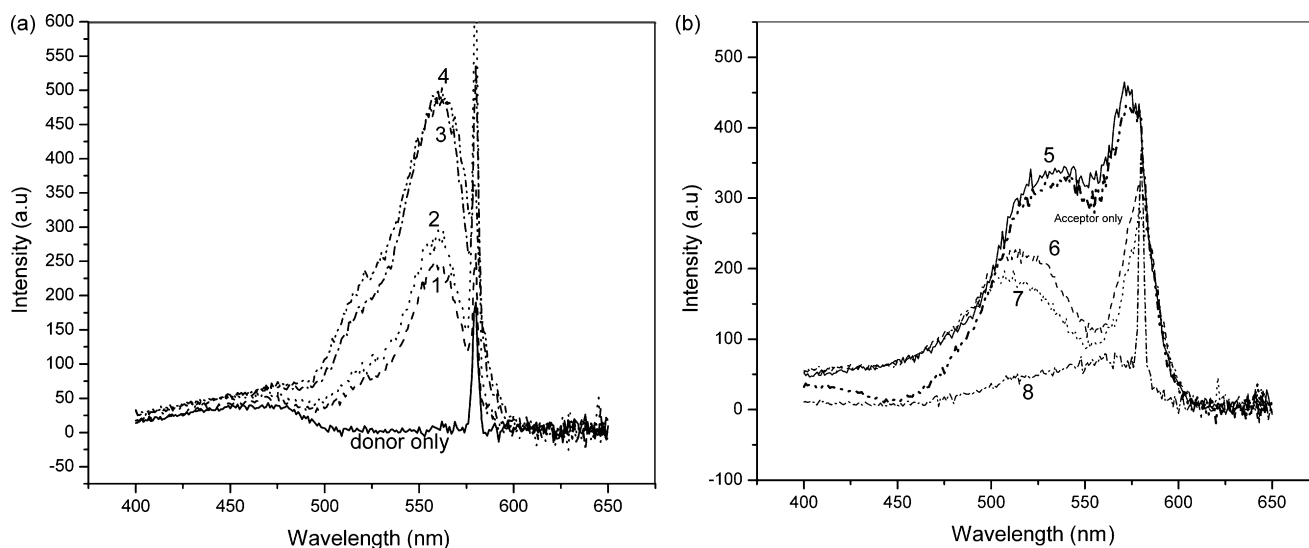


Fig. 5. (a) Excitation spectra of dye mixture doped PMMA for 580 nm emission. (1) $[A] = 4 \times 10^{-5}$ m/l, (2) $[A] = 7 \times 10^{-5}$ m/l, (3) $[A] = 10^{-4}$ m/l and (4) $[A] = 2 \times 10^{-4}$ m/l. (b) Excitation spectra of dye mixture doped PMMA for 580 nm emission. (5) $[A] = 4 \times 10^{-4}$ m/l, (6) $[A] = 5 \times 10^{-4}$ m/l, (7) $[A] = 6 \times 10^{-4}$ m/l and (8) $[A] = 7 \times 10^{-4}$ m/l.

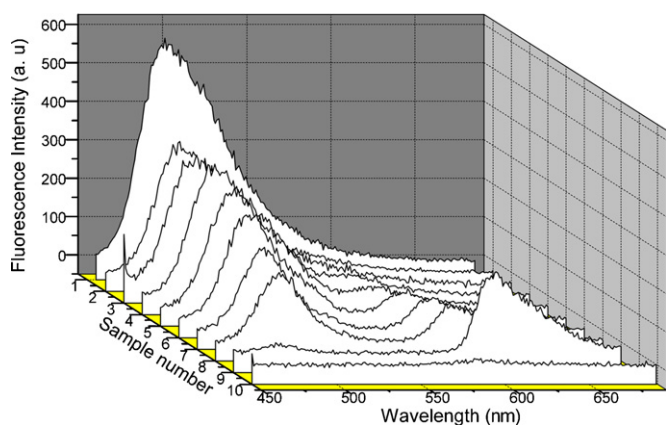


Fig. 6. The recorded fluorescence from dye mixture doped PMMA with 445 nm excitation. Sample 1: donor only, sample 2: $[A] = 4 \times 10^{-5}$ m/l, sample 3: $[A] = 7 \times 10^{-5}$ m/l, sample 4: $[A] = 10^{-4}$ m/l, sample 5: $[A] = 2 \times 10^{-4}$ m/l, sample 6: $[A] = 4 \times 10^{-4}$ m/l, Sample 7: $[A] = 5 \times 10^{-4}$ m/l, Sample 8: $[A] = 6 \times 10^{-4}$ m/l, sample 9: $[A] = 7 \times 10^{-4}$ m/l and sample 10: acceptor only (10^{-4} m/l).

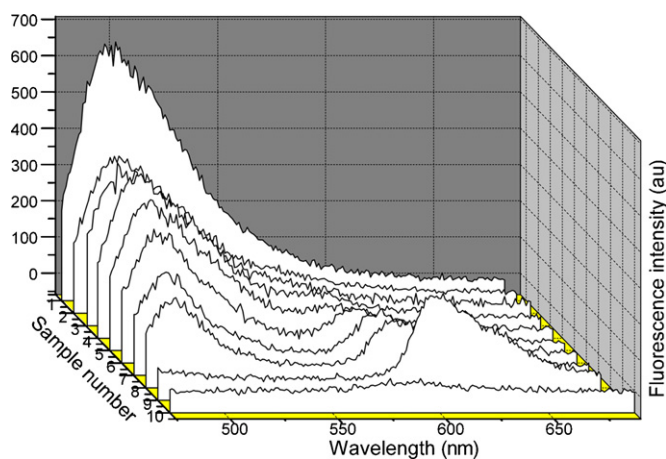


Fig. 7. The recorded fluorescence from dye mixture doped PMMA with 465 nm excitation. Sample 1: donor only, sample 2: $[A] = 4 \times 10^{-5}$ m/l, sample 3: $[A] = 7 \times 10^{-5}$ m/l, sample 4: $[A] = 10^{-4}$ m/l, sample 5: $[A] = 2 \times 10^{-4}$ m/l, sample 6: $[A] = 4 \times 10^{-4}$ m/l, sample 7: $[A] = 5 \times 10^{-4}$ m/l, sample 8: $[A] = 6 \times 10^{-4}$ m/l, sample 9: $[A] = 7 \times 10^{-4}$ m/l, sample 10: acceptor only (10^{-4} m/l).

5. Energy transfer rate constants

The excitation wavelength dependence of energy transfer efficiency and the transfer rate constant for the present system can be calculated by studying the relative fluorescence intensities of the donor (I_{0d}/I_d) at various excitation wavelengths. As seen in Fig. 11, there is a noticeable change in the slope of the Stern–Volmer plot for the 488 nm excitation. At this wavelength, the donor emission was found to be rapidly quenched by the acceptor. In the present study, the maximum value of radiative energy transfer rate constant was found to be $6.6 \times 10^{11} \text{ s}^{-1}$ with an excitation wavelength 465 nm. The rate constants for 445 and 488 nm excitations were 5.4×10^{11} and $3.5 \times 10^{11} \text{ s}^{-1}$, respectively. This result is attributed to the fact that, both 445 and 465 nm, excitations come well outside the donor emission while 488 nm is partly absorbed by both donor and acceptor. This is clear from the excitation spectra at 495 nm, which shows finite absorption at 488 nm by the samples. Thus the calculated parameters for the dye mixture with 488 nm may vary much from the values for the other two wavelengths of excitation.

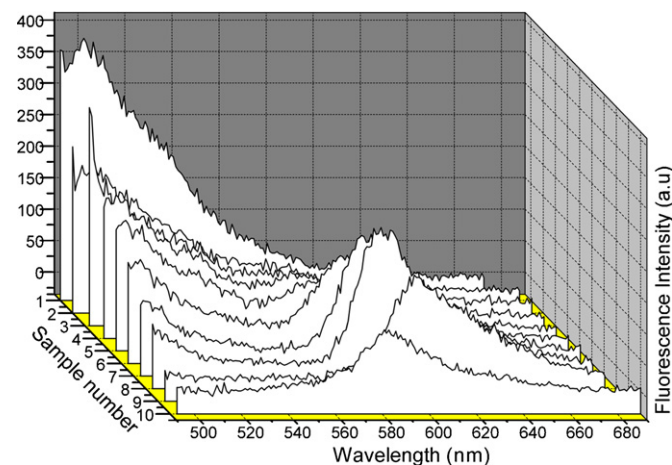


Fig. 8. The recorded fluorescence from dye mixture doped PMMA with 488 nm excitation. Sample 1: donor only, sample 2: $[A] = 4 \times 10^{-5}$ m/l, sample 3: $[A] = 7 \times 10^{-5}$ m/l, sample 4: $[A] = 10^{-4}$ m/l, sample 5: $[A] = 2 \times 10^{-4}$ m/l, sample 6: $[A] = 4 \times 10^{-4}$ m/l, sample 7: $[A] = 5 \times 10^{-4}$ m/l, sample 8: $[A] = 6 \times 10^{-4}$ m/l, sample 9: $[A] = 7 \times 10^{-4}$ m/l and sample 10: acceptor only (10^{-4} m/l).

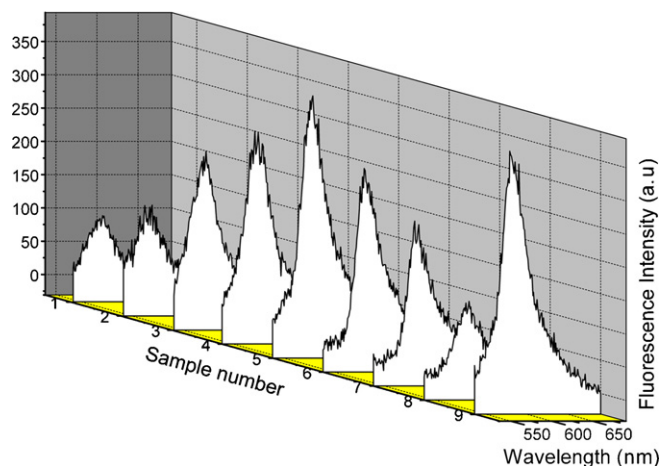


Fig. 9. The recorded fluorescence from dye mixture doped PMMA with 532 nm excitation. Sample 1: $[A] = 4 \times 10^{-5}$ m/l, sample 2: $[A] = 7 \times 10^{-5}$ m/l, sample 3: $[A] = 10^{-4}$ m/l, sample 4: $[A] = 2 \times 10^{-4}$ m/l, sample 5: $[A] = 4 \times 10^{-4}$ m/l, sample 6: $[A] = 5 \times 10^{-4}$ m/l, sample 7: $[A] = 6 \times 10^{-4}$ m/l, sample 8: $[A] = 7 \times 10^{-4}$ m/l and sample 9: acceptor only (10^{-4} m/l).

Knowing the value of $[A]_{1/2}$ the half quenching concentration at which $I_d = I_{od}/2$, the values of the critical radii R_0 can be evaluated [11]. The values obtained for R_0 clearly shows that the non-radiative transfer involved in the dye mixture is of dipole-dipole in nature.

The fluorescence lifetime of the pure donor was measured experimentally using time correlated single photon counting technique. Fig. 12 shows the fluorescence decay curve of the donor, which gives lifetime of the donor in the absence of the acceptor as 4.99 ns when embedded in PMMA. Also a very little decrease in the lifetime was noticed due to the presence of acceptor, which is a signature of radiative type of energy transfer in the rods. Fig. 13 shows the decay curve of the donor in the presence of acceptor (7×10^{-4} m/l) giving a lifetime of 4.83 ns.

Using this value of τ_{od} , the total energy transfer rate constant K_T is calculated and a comparison between the radiative and non-radiative contributions to the energy transfer can be made by plotting a graph between η_r/η_{nr} and $[A]$.

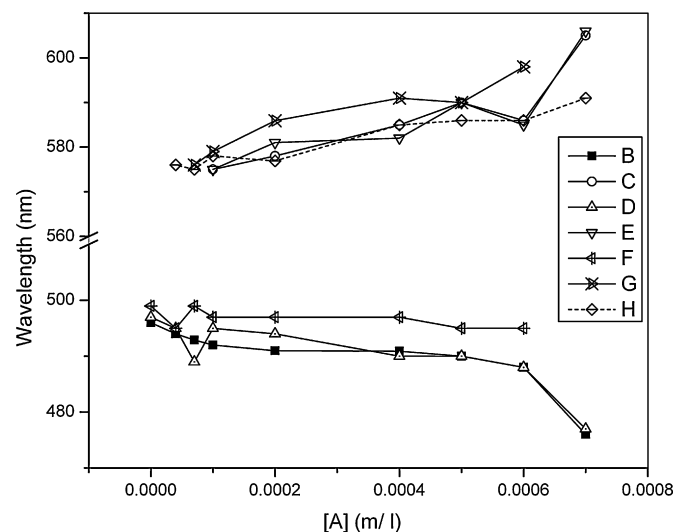


Fig. 10. Simultaneous peak emission wavelengths available from the rods fabricated with different acceptor concentrations. (B) Donor emission at 445 nm excitation, (C) acceptor emission at 445 nm excitation, (D) donor emission at 465 nm excitation, (E) acceptor emission at 465 nm excitation, (F) donor emission at 488 nm excitation, (G) acceptor emission at 488 nm excitation and (H) emission at 532 nm excitation.

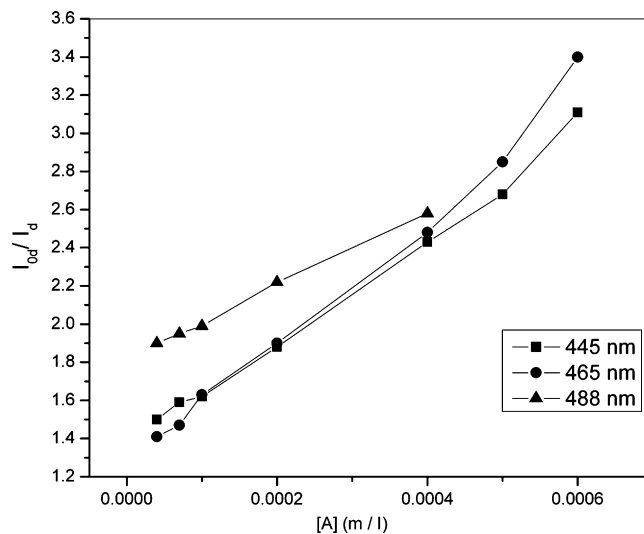


Fig. 11. The Stern-Volmer plot for the present ETDL system.

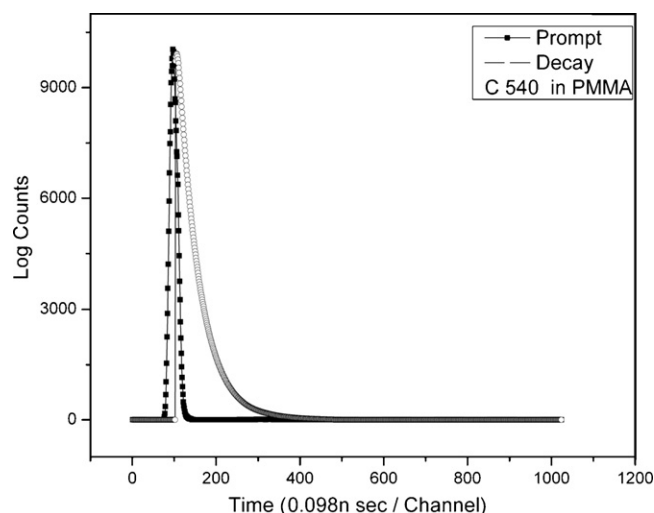


Fig. 12. The fluorescence decay curve of the donor C 540 in PMMA matrix.

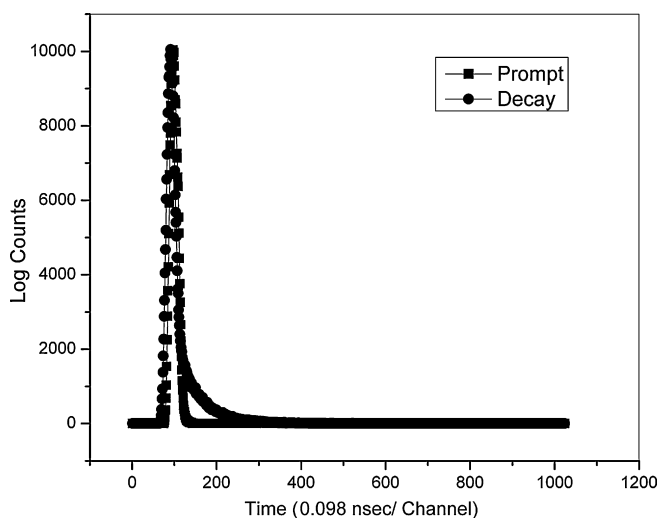


Fig. 13. The fluorescence decay curve of the donor C 540 in the presence of Rh B (10^{-5} m/l) in PMMA matrix.

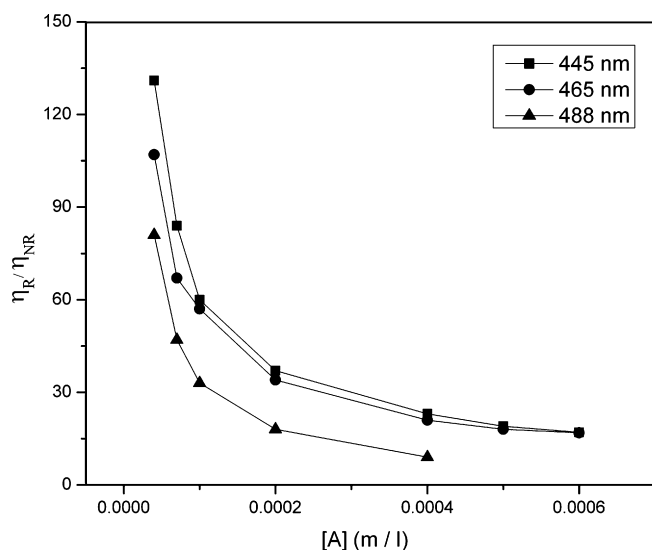


Fig. 14. Plot of η_r/η_{nr} vs. $[A]$.

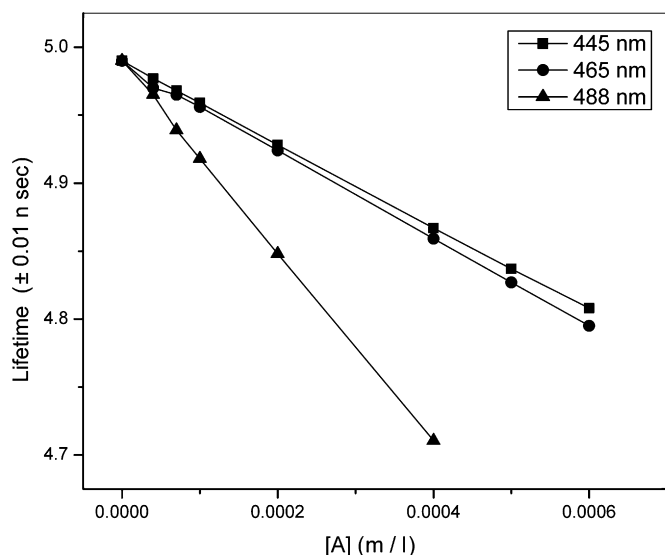


Fig. 15. Variation of donor lifetime with $[A]$.

Fig. 14 shows such a graph and the minimum value of the ratio η_r/η_{nr} was found to be ~ 9 occurring at 488 nm excitation. The result clearly indicates that, at all the three wavelengths of excitation, non-radiative transfer part is comparatively less important than the radiative transfer mechanism in the present ETDL system even though the non-radiative part shows an increase in its values at higher acceptor concentrations.

By knowing the values of τ_{0d} and ϕ_{0d}/ϕ_d , the value of τ_d , the fluorescence lifetime of the donor in the presence of acceptor at various acceptor concentrations can be evaluated. Fig. 15 shows the graph between lifetime and acceptor concentration. Again, for 488 nm excitation, the calculated donor lifetime 4.71 ns with $[A] = 7 \times 10^{-4}$ m/l is shorter than the experimentally measured

Table 1
Calculated parameters of the dye mixture doped preforms

Parameter	445 nm	465 nm	488 nm
$K_r (\times 10^9 \text{ s}^{-1})$	542	661	355
$K_{nr} (\times 10^9 \text{ s}^{-1})$	12	13	29
$R_0 (\text{\AA})$	116.3	119	154
$[A]_{1/2} (\times 10^{-4} \text{ M})$	2.52	2.35	1.07
$\tau_d (\times 10^{-9} \text{ s})$ (at $[A] = 7 \times 10^{-4} \text{ M}$)	4.808	4.795	4.711

value while for the other two excitation wavelengths, the calculated values are around 4.8 ns which agrees with the measurement. With 445 and 465 nm excitations, nonradiative relaxations taking place in the S_1 manifold before the energy gets transferred to the acceptor can result in a longer lifetime. Such relaxations may not be that much important in the case of 488 nm excitation resulting in rapid energy transfer. The results clearly show the importance of the selection of the excitation wavelength in the context of the energy transfer studies. Table 1 summarises the various calculated parameters of the dye mixture doped rods for the three excitation wavelengths.

6. Conclusions

We have analysed the excitation wavelength dependence of the fluorescence emission from C 540–Rh B dye mixture system in PMMA rods. For the pump wavelengths 445 and 465 nm, many of the fabricated rods emit at two peak wavelengths simultaneously. A comparable relative intensity for the simultaneous peak emission wavelengths was observed from a rod with acceptor concentration 6×10^{-4} m/l when excited with 445 and 465 nm whereas for a 488 nm excitation, the rod with acceptor concentration 4×10^{-4} m/l exhibits such a property. These rods can also offer single peak emission outputs ranging from 576 to 591 nm with a frequency-doubled Nd:YAG laser excitation. Calculated parameters at 445 and 465 nm excitation are in close agreement with the experimental results.

References

- [1] A.J. Cox, B.K. Matisse, Chem. Phys. Lett. 76 (1) (1980) 125–128.
- [2] S. Sinha, A.K. Ray, S. Kundu, Sasikumar, T.B. Pal, S.K.S. Nair, K. Dasgupta, Appl. Opt. 41 (2002) 7006–7011.
- [3] D.J. Taylor, S.E. Harris, S.T.K. Nieh, T.W. Hansch, Appl. Phys. Lett. 19 (1971) 269–271.
- [4] E.F. Zalewski, R.A. Keller, Appl. Opt. 10 (1971) 2773–2775.
- [5] H.S. Pilloff, Appl. Phys. Lett. 21 (1972) 339–340.
- [6] G.A. Kumar, V. Thomas, G. Jose, N.V. Unnikrishnan, V.P.N. Nampoori, J. Photochem. Photobiol. A 153 (2002) 145–151.
- [7] M. Kailasnath, T.S. Sreejaya, R. Kumar, P. Radhakrishnan, V.P.N. Nampoori, C.P.G. Vallabhan, J. Opt. Laser Tech. 40 (2008) 687–691.
- [8] G.D. Peng, Z. Xiong, P.L. Chu, J. Lightwave Technol. 16 (1998) 2365–2372.
- [9] M. Kailasnath, P.R. John, P. Radhakrishnan, V.P.N. Nampoori, C.P.G. Vallabhan, J. Photochem. Photobiol. A: Chem. 195 (2008) 135–143.
- [10] G.A. Kumar, N.V. Unnikrishnan, J. Photochem. Photobiol. A: Chem. 144 (2001) 107–117.
- [11] J.R. Lakowicz, Principles of Fluorescence Spectroscopy, 3rd ed., Springer, 2006.
- [12] S. Speiser, R. Katrarro, Opt. Commun. 27 (1978) 287–291.
- [13] M.A. Ali, S.A. Ahmed, Appl. Opt. 29 (1990) 4494.
- [14] J.B. Birks, M.S.S.C.P. Leite, J. Phys. B 3 (1970) 513.
- [15] T. Govindanunni, B.M. Sivaram, J. Lumin. 21 (1980) 397.
- [16] M. Rajesh, K. Geetha, C.P.G. Vallabhan, P. Radhakrishnan, V.P.N. Nampoori, Appl. Opt. 46 (1) (2007) 106–112.
- [17] T. Urisu, K. Kajiyama, J. Appl. Phys. 47 (1976) 3563–3565.
- [18] P.J. Sebastian, K. Sathyanandan, Opt. Commun. 35 (1980) 113–114.